Surface Chemistry

DOI: 10.1002/anie.200701117

Forming Aromatic Hemispheres on Transition-Metal Surfaces**

Kwang Taeg Rim, Mohamed Siaj, Shengxiong Xiao, Matthew Myers, Vincent D. Carpentier, Li Liu, Chaochin Su, Michael L. Steigerwald, Mark S. Hybertsen, Peter H. McBreen, George W. Flynn, and Colin Nuckolls**

This study details a new method to create materials by integrating polycyclic aromatic hydrocarbons into reactive transition-metal surfaces. We describe the interaction of hexabenzocoronene (**1**, HBC, Figure 1a)[1] with a clean ruthenium surface. Interest in **1** and its interaction with transition-metal surfaces is driven by its relationship to the end cap of a carbon nanotube, to polynuclear aromatic hydrocarbons,[2–8] and to reactor carbonization.[9] Even though **1** is a large and multifunctional molecule, its high symmetry (there are only five types of C atom) simplifies the interpretation of the fundamental surface-molecule chemistry. Ruthenium provides a catalytically active metal that is capable of π bonding to polycyclic aromatic hydrocarbons and is known to be active in many processes such as Fischer–Tropsch[10] and olefin metathesis.[11]

Our experimental approach utilizes a combination of scanning tunneling microscopy (STM),[12–14] reflectance absorbance infrared spectroscopy (RAIRS), and temperature-programmed desorption (TPD)[15] to study the surface chemistry of **1**. Before depositing **1**, we cleaned the (0001) face of a Ru crystal by repeated cycles of Ar^+ sputtering, annealing in oxygen at around 940 °C, and then annealing at 1100 °C. STM images of the crystal prior to chemisorption show large flat terraces (ca. 100 nm wide) in which the individual atoms could be resolved. One of these images is shown in Figure S1 A in the Supporting Information. There are a few larger bright features that apparently resulted from underlying damage to the Ru crystal by sputtering and annealing (Figure S1 B). Despite these sparse defects, the arrangement of surface atoms is essentially unaffected. These features had no measurable effect on the surface chemistry or spectroscopy described below. Furthermore, the low-energy electron diffraction (LEED) pattern at 59 eV showed a hexagonally close-packed 1×1 arrangement, as expected for the (0001) surface. No significant amount of surface oxygen atoms was detected by Auger spectroscopy. It is difficult to quantify by Auger electron spectroscopy how much carbon is on the surface, but the amount must be relatively low in view of the high quality of the STM image (Figure S1). Moreover, minor impurities on the surface will not affect the experiments because the surfaces are covered with substantially less than a monolayer of **1**.

Figure 1 shows the STM measurements of **1** on the Ru single crystal at a base pressure of 3×10^{-10} Torr and at room temperature.[16,17] The features on the surface are hexagonally shaped. We measured the width of these features from the full width at half maximum in the topographic images to counteract tip effects, which tend to inflate the lateral size of molecules on the surface of metals. The diameter of **1** measured in Figure 1d (1.5 ± 0.1 nm) is slightly larger than the diameter of **1** (ca. 1.4 nm) measured from its crystal structure. The important conclusion is that **1** bonds "face-on" to the Ru(0001) surface.

We observed no mobility of the molecules on the surface of ruthenium over duration of the experiment (typically several hours). By contrast, we observed high mobility of

[*] K. T. Rim, M. Siaj, S. Xiao, M. Myers, L. Liu, M. L. Steigerwald, Prof. G. W. Flynn, Prof. C. Nuckolls
Department of Chemistry and
The Center for Electron Transport in Molecular Nanostructures
Columbia University
New York, NY 10027 (USA)
Fax: (+1) 212-932-1289 (C.N.) or (+1) 212-854-8336 (G.W.F.)
E-mail: gwf1@columbia.edu
cn37@columbia.edu
Homepage: nuckolls.chem.columbia.edu

V. D. Carpentier, P. H. McBreen
Department de Chemie
Universite Laval
Quebec, QC, G1K 7P4 (Canada)

C. Su
Department of Molecular Science and Engineering
National Taipei University of Technology
Taipei 106 (Taiwan)

M. S. Hybertsen
Center for Functional Nanomaterials
Brookhaven National Laboratory
Upton, NY 11973-5000 (USA)

[**] This work was funded by the Department of Energy under Grant No. DE-FG02-88ER13937 (G.W.F.). Equipment support provided by the National Science Foundation under grant CHE-03-52582 (G.W.F.). We acknowledge financial support from the Nanoscale Science and Engineering Initiative of the National Science Foundation under NSF Award Number CHE-0117752 and by the New York State Office of Science, Technology, and Academic Research (NYSTAR). We acknowledge support from the Chemical Sciences, Geosciences and Biosciences Division, Office of Basic Energy Sciences, US D.O.E. (DE-FG02-01ER15264). C.N. thanks the Alfred P. Sloan Fellowship Program (2004). We thank the MRSEC Program of the National Science Foundation under Award Number DMR-0213574 and by the New York State Office of Science, Technology and Academic Research (NYSTAR) for financial support for MLS and the shared instrument facility. We acknowledge research support from the Natural Sciences and Engineering Research Council (NSERC) of Canada. M.S. acknowledges the receipt of an NSERC postdoctoral scholarship.

Supporting information for this article (experimental and theoretical methods, STM images, current–voltage characteristics, RAIRS spectrum, and computed structures/frontier orbitals for **3**) is available on the WWW under http://www.angewandte.org or from the author.

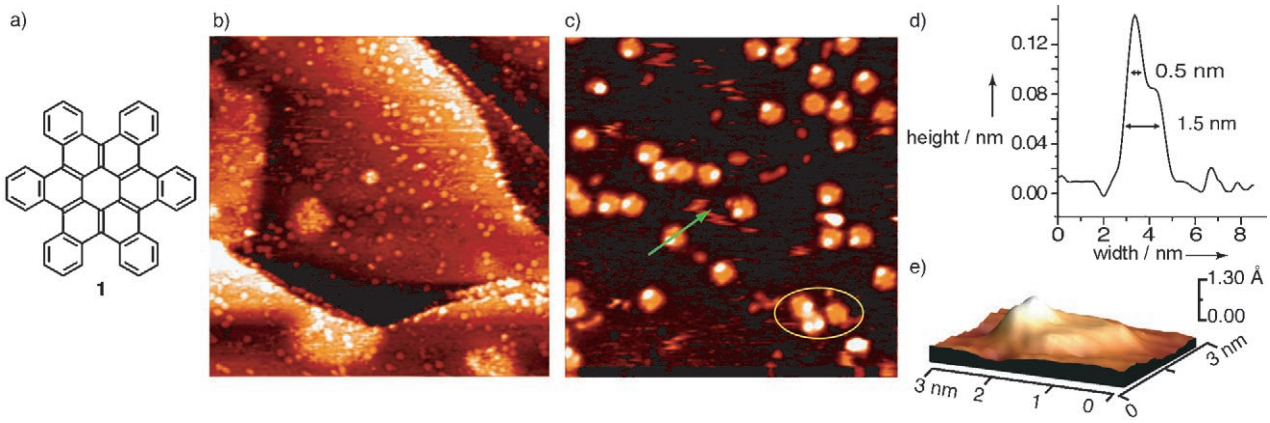

Figure 1. a) Structure of HBC (**1**). b) STM topograph of HBC on Ru (80×80 nm^2) recorded at $+1.9$ V, 0.1 nA, and room temperature. c) Constant-current STM image (26.5×26.5 nm^2) of HBC molecules obtained at -0.7 V and 0.1 nA. The yellow oval surrounds the three different types of molecular morphologies observed. d) Line profile along the green arrow in (c) showing the width of the molecule (1.5 ± 0.1 nm), the diameter of the brightest spot in the molecular image (0.5 ± 0.1 nm), and the height difference between the brightest spot and the molecular plane (0.52 ± 0.08 Å). e) 3D STM image ($3\times3\times0.13$ nm^3) for one of the hexagonal features in the oval in (c).

these molecules on the surface of graphite.[17] The electronic structure of **1** dictates that the central six-membered ring has double bonds radiating out from the molecular center as in the resonance structure shown in Figure 1 a.[18] These type of diene-like fragments are known to bind to transition metals.[19] We propose that the ruthenium is bound strongly to the HBC through these diene functions, and this binding is further strengthened by interaction between the remainder of the π system and the metal surface. Density functional theory (DFT) simulations[20] (see the Supporting Information for theoretical methods) support that the strongest initial binding between ruthenium metal and the HBC occurs at the diene-like portion of the molecule. We used the complex $[Ru(PH_3)_3]$ as a computationally tractable source of low-valent ruthenium and determined its optimized, lowest energy complex with the **1** (Figure 2 a,b); the metal atom is situated under the diene section of the HBC. This isolated ruthenium atom is not used to approximate the surface but rather to show where low-valent ruthenium would bond most strongly. On the surface, the molecule will enjoy multiple contacts.

The yellow oval in Figure 1 c highlights three different molecular topographies for **1** on the surface of ruthenium. One has a prominent bright feature, decidedly off-center within each of the molecules in the STM micrographs of **1** on the surface of ruthenium. Another one has essentially uniform electron density across the molecule. The third type of topography has two of these bright features. These bright spots are constant in size (ca. 0.5 nm in diameter) over many different molecules. The majority (80 %) of the molecules on the surface have only one of these bright features. Figure 1 d shows a line profile across one of these features (along the green arrow in Figure 1 c). A three-dimensional view of the STM image of one molecule (with only one bright feature) reveals a camelback shape (Figure 1 e). These bright features in the STM images could result from flattening of portions of the molecule on the surface, adatoms, hydrogen vacancies, or a partial dehydrogenation on the metal surface. Regardless of the origin of these features and in view of the low mobility of the molecules on the surface, we conclude that the molecules

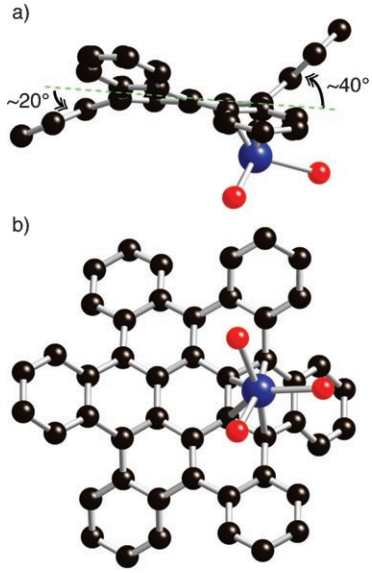

Figure 2. a,b) Two views of the lowest-energy geometry for [HBC–$Ru(PH_3)_3$] as determined by DFT simulations (blue Ru, red P). For clarity, the hydrogen atoms are not shown. The angles are those between the planes of the central and outer six-membered rings.

are bound very strongly[1] to the substrate and that the carbon framework of **1** is essentially intact.

In view of the bonding of the HBC to the surface, the catalytic reactivity of ruthenium towards hydrogenation, dehydrogenation, and hydrogen-transfer reactions could be exploited.[22] The reaction on the surface could proceed through the oxidative addition to neighboring aryl C–H bonds,[10,23] removal of two H atoms (either as H_2 or as metal hydrides), and the formation of a C–C bond to give a five-membered ring. For 4-helicene, this process is known to occur for heterogeneous, transition-metal catalysts.[24] Moreover, Weiss et al.[23] observed the dehydrogenation of hexaphenylbenzene to a planar aromatic hydrocarbon on the Cu(111) surface.

The fate of HBC adsorbed on Ru(0001) was studied by TPD. HBC was adsorbed at room temperature, and then the sample was heated to 1200 K at a constant heating rate of 1 K s^{-1}. Figure 3 a shows the desorption of H_2 to give TPD peaks at around 380 and 414 K, as well as a broad peak from 475 to 700 K. The dehydrogenation of HBC occurs over a large temperature range, which is consistent with a number of previous studies of adsorption and dissociation of unsaturated hydrocarbons on Ru surfaces. It is particularly important to consider data reported by Jakob and Menzel, as well as Koschel et al. for the interaction of benzene with Ru(0001).[25–27] They observe a stepwise dehydrogenation that begins at 400 K and continues to 750 K. Moreover, similar reactions and desorption peaks are seen with C_2H_2,[28] C_2H_4,[29] and C_6H_6[25,26] on Ru surfaces ($T = 540$, 605–622, 678 K for desorbing hydrogen). However, TPD studies for H_2 alone on the Ru surface show desorption peaks at 320 and 380 K.[30,31] This result indicates that **1** could partially dehydrogenate at around 380 K, thereby providing the high adsorption stability of HBC.

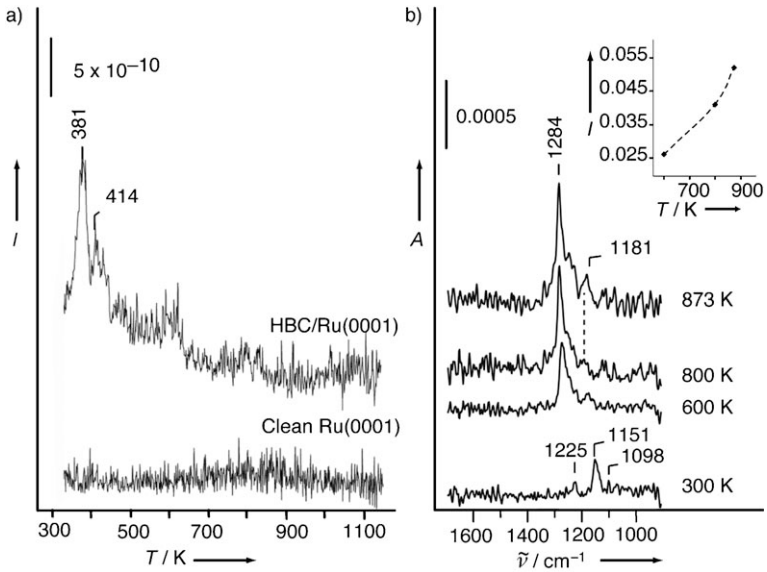

Figure 3. Thermal behavior of **1**–Ru. a) Thermal desorption spectra of H_2 from adsorbed HBC on clean Ru(0001) (top) and of clean Ru (0001) without HBC (bottom). b) Reflectance infrared (RAIRS) spectra recorded at 100 K following annealing of HBC exposed Ru(0001) to the indicated temperatures; inset: integrated band (1284 cm^{-1}) intensity as function of heating temperature. I = integrated intensity.

Infrared reflectance spectra (Figure 3 b) of a HBC monolayer adsorbed on Ru(0001) at room temperature display bands at 1098, 1151, and 1225 cm^{-1}, which can be attributed to mixed C–H bending and C–C stretching modes of a polycyclic hydrocarbon.[32,33] When the sample is heated to 600 K and above, a strong band at 1284 cm^{-1} and a weaker band at 1181 cm^{-1} develop. Both bands are close to the values for C–C stretching modes of benzene and vinylidene on Ru(0001), respectively.[25,34] Furthermore, both the IR spectra of benzo[*a*]pyrenes[32] and the surface-enhanced Raman scattering (SERS) spectra of nitro polycyclic aromatic hydrocarbon complexes[33] display bands in the 1300–1000-cm^{-1} region. These bands are assigned to C–H in-plane deformation modes (δ(CH)) and C–C stretching motions coupled with the ring C-C-H bending modes. Over this temperature range, the intensity of the RAIRS bands change considerably; the intensity of the ν(C–C) band (1284 cm^{-1}) increases (Figure 3 b, inset). The metal-surface selection rule[35] varies as $\cos^2\theta$ (θ = angle between the surface normal and the transition dipole). Hence, growth of the band at 1284 cm^{-1} with increasing temperature indicates that the C–C bonds bend further away from the surface with increasing temperature. The infrared data are in good agreement with the STM results (see below) showing an increase in the apparent height of the adsorbate (ca. 0.1 to ca. 0.2 nm) upon heating. In general, this behavior is what is expected for dehydrogenation of an aromatic ring on ruthenium to produce an upright aromatic ring.

Figure 4 a,b shows STM images (recorded at room temperature) of the HBC/Ru surface after it had been heated to around 873 K for 15 minutes. Neither the STM images nor the IR spectra change further up to 1200 K (see Figure S5 in the Supporting Information), indicating that the product is stable and remains intact. The large circular bright features, subsurface damage during sample preparation, are present in the pristine Ru surface before dosing with molecules. Eighty percent of the molecules on the surface are isolated and monomeric. For these structures, the thermal process gives a single dominant product that is quite symmetrical: approximately 90 % of the monomer STM topographs are geometrically identical and essentially circular. Given that these features are consistently the same size and shape, it seems unlikely that these features are agglomerates of multiple atoms or simply nonuniform clusters of carbon. The structures on the surface of ruthenium are physically coupled very strongly, as they do not show any surface mobility when they are scanned repeatedly by STM.

The apparent diameter of the isolated molecules decreased (relative to **1**) to 1.1 ± 0.2 nm (Figure 4 c). The off-center bright spots in the initial, unheated sample are absent, and the bright features are centered on the molecule but diffuse. Comparison of 3D STM images (Figure 1 d and Figure 4 d) shows a clear change. In addition, a comparison of the current–voltage curves (Figure S4 in the Supporting Information) taken over the HBC features reveals a significant increase in conductivity after reaction. As a point of emphasis, whereas the IR data in Figure 3 show that the aromatic ring is more upright, the structure in the STM image is symmetric. The implication is that all of the edge carbon atoms in this model would be bonded similarly and more upright, but not fully upright.

We do not have an unequivocal structure of the molecule after heating. We examined the structures and energetics of the molecular species that result from the cyclodehydroge-

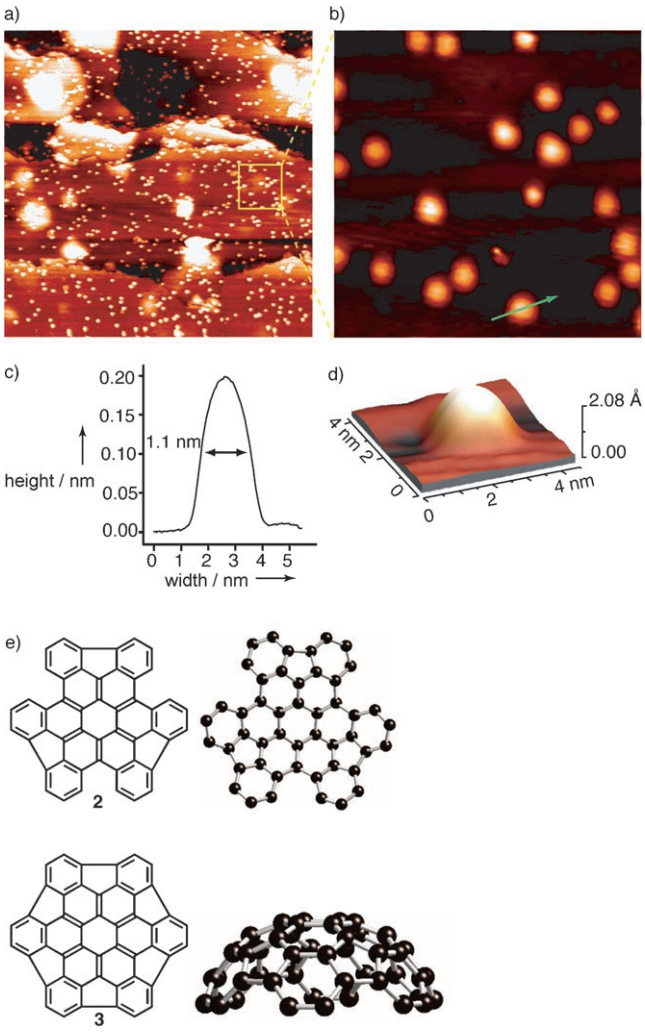

Figure 4. a) STM topographic image (150×150 nm^2) obtained at +1.7 V, 0.3 nA, and room temperature after annealing HBC on the ruthenium surface at 600 °C. b) Expanded image of the area indicated by the yellow box in (a). c) Line profile along the green arrow in (b) passing through a molecular feature with a diameter of 1.1 ± 0.2 nm. d) 3D STM image (4×4 nm^2) for annealed product showing a bowl-shaped, rim-down surface species. e) Models for two stages in the hypothesized evolution during annealing: a nearly flat isomer with three five-membered rings (**2**) and a completely dehydrogenated HBC (**3**).

nation of molecule **1** through DFT calculations.[20] There are 12 possible structures. In these reactions, one such dehydrogenative cyclization gives only one possible isomer, two cyclizations gives three possible isomers, three cyclizations gives three isomers, four cyclizations gives three isomers, five cyclizations gives one isomer, and six cyclizations gives one isomer (structural and thermochemical results are included in the Supporting Information). The incorporation of these smaller-sized rings changes the shape of the HBC considerably. Two of these structures are shown in Figure 4. One of them (**2**) is essentially flat. Further ring formation to yield six five-membered rings creates a hemispherical chemical structure (**3**). The first three ring closures (to form **2**) are isoenergetic (+23 kcal mol^{-1}). Upon the formation of the fourth five-membered ring, the structure begins to buckle, which provides significant ring strain and makes this ring formation the most energetically unfavored. After this, the fifth and sixth ring closures require less energy than the fourth. These reactions also are calculated to be endothermic, but the associated surface-mediated reactions are certainly plausible in view of the high reaction temperature and inasmuch as the H_2 assumed in our model calculations is a high-energy by-product. (For example, the dissociative adsorption of H_2 to the metal surface could provide sufficient energy to promote each of the dehydrogenative cyclizations.)

Of the 12 structures examined by DFT above, we consider only **2** and **3** as possibilities for the reaction product as they are the only symmetric structures consistent with the images in Figure 4. At higher bias voltages, the features do not change substantially (Figure S3 in the Supporting Information). Under either tunneling-in or tunneling-out conditions, the bright spot remains in the center of the structure. This result indicates that both the occupied and the unoccupied frontier orbitals must be symmetrical and have substantial amplitude at the center of the molecule. The frontier orbitals of **3** are shown in Figure S7 in the Supporting Information. The strong physical coupling of these species with the surface provides a strong electronic coupling and should substantially broaden these energy levels. This point is magnified by the propensity of Ru to form multiple bonds with carbon, providing strong electronic coupling with the surface.[10,11] Of the computed structures, only the frontier orbitals of **2** or **3** satisfy the requirement of being symmetrical. However, the size of the adsorbate is more consistent with a rim-down bowl-shaped adsorbate rather than the flat structure **2** (Figure 4e). Although the diameter of the product is smaller than that of the unheated adsorbate (1.1 ± 0.2 nm vs. 1.5 ± 0.1 nm), the height is greater (0.2 ± 0.02 vs. 0.10 ± 0.02 nm). If **2** had formed, the diameter should increase and the height should decrease. A species such as **3** with its higher profile structure agrees well with the IR measurements, which show an increase in intensity upon dehydrogenation. The C–C ring stretches of **2** should be extremely weak.

The structure of the hydrocarbon **3** ($C_{48}H_{12}$) and the energetics of its formation from **1** suggest to us that the ultimate product we observe is the fully dehydrogenated hemispherical adduct C_{48}. This adduct would be very strongly bound to the Ru surface by at least 12 Ru–C σ bonds, and therefore the electronic coupling between the metal and the organic moiety would be substantial.

We have presented a method for joining polycyclic aromatic hydrocarbons to transition-metal surfaces. Compound **1** binds to the surface of the ruthenium crystal. When the HBC–surface complex is heated, hydrogen is evolved. We suggest that the product species is a bowl-shaped molecular fragment that is strongly bound, rim down, to the metal surface. This structure is significant because it represents a new type of seed that has the capacity to grow a single-walled carbon nanotube of specific diameter and chirality by addition of carbon atoms to this transition-metal-bound fragment. Furthermore, the behavior of HBC on Ru high-

lights the importance of metal atoms as potential catalysts in soot-forming combustion reactions.[36,37]

Received: March 14, 2007
Revised: August 22, 2007
Published online: September 18, 2007

Keywords: carbon · nanostructures · nanotubes · polycycles · surface chemistry

[1] S. Xiao, M. Myers, Q. Miao, S. Sanaur, K. Pang, M. L. Steigerwald, C. Nuckolls, *Angew. Chem.* **2005**, *117*, 7556; *Angew. Chem. Int. Ed.* **2005**, *44*, 7390.
[2] A. G. Robinson, P. R. Winter, C. Ramos, T. S. Zwier, *J. Phys. Chem. A* **2000**, *104*, 10312.
[3] A. G. Robinson, P. R. Winter, T. S. Zwier, *J. Phys. Chem. A* **2002**, *106*, 5789.
[4] C. S. McEnally, L. D. Pfefferle, *Combust. Flame* **1998**, *115*, 81.
[5] J. Appel, H. Bockhorn, M. Frenklach, *Combust. Flame* **2000**, *121*, 122.
[6] M. Frenklach, *Phys. Chem. Chem. Phys.* **2002**, *4*, 2028.
[7] H. Richter, O. A. Mazyar, R. Sumathi, W. H. Green, J. B. Howard, J. W. Bozzell, *J. Phys. Chem. A* **2001**, *105*, 1561.
[8] H. F. Calcote, *Combust. Flame* **1981**, *42*, 215.
[9] C. D. Tan, R. T. K. Baker, *Catal. Today* **2000**, *63*, 3.
[10] J. P. Collman, L. S. Hegedus, J. R. Norton, R. G. Finke in *Principles and Applications of Organotransitionmetal Chemistry*, University Science Books, **1987**, p. 279.
[11] R. H. Grubbs in *Handbook of Olefin Metathesis*, Wiley, New York, **2002**, p. 61.
[12] G. M. Florio, T. L. Werblowsky, T. Mueller, B. J. Berne, G. W. Flynn, *J. Phys. Chem. B* **2005**, *109*, 4520.
[13] M. Lackinger, S. Griessl, W. M. Heckl, M. Hietschold, G. W. Flynn, *Langmuir* **2005**, *21*, 4984.
[14] T. Mueller, T. L. Werblowsky, G. M. Florio, B. J. Berne, G. W. Flynn, *Proc. Natl. Acad. Sci. USA* **2005**, *102*, 5315.
[15] S. Lavoie, P. McBreen, *J. Phys. Chem. B* **2005**, *109*, 11986.
[16] K. T. Rim, T. Muller, J. P. Fitts, K. Adib, N. Camillone III, R. M. Osgood, E. R. Batista, R. A. Friesner, S. A. Joyce, G. W. Flynn, *J. Phys. Chem. B* **2004**, *108*, 16753.
[17] K. T. Rim, L. Liu, C. Su, M. S. Hybertsen, G. W. Flynn, unpublished results.
[18] Y. S. Cohen, S. Xiao, M. L. Steigerwald, C. Nuckolls, C. R. Kagan, *Nano Lett.* **2006**, *6*, 2838.
[19] M. A. Bennett, M. Bown, D. C. R. Hockless, *Aust. J. Chem.* **2000**, *53*, 507.
[20] The frontier orbitals of **3** are shown in theSupporting Information. The molecular DFT calculations were performed by using Jaguar (versions 6.0 and 6.5) with the B3LYP functional: Schrodinger, L. L. C., Portland, OR, **1991–2005**. The surface DFT calculations were performed with the PBE functional by using ABINIT. The ABINIT code is a common project of the Université Catholique de Louvain, C. I., and other contributors. URL: http://www.abinit.org. See: X. Gonze, et al., *Comput. Mater. Sci.* **2002**, *25*, 478.
[21] D. B. Dougherty, P. Maksymovych, J. T. Yates, Jr., *Surf. Sci.* **2006**, *600*, 4484.
[22] T. Naota, H. Takaya, S.-I. Murahashi, *Chem. Rev.* **1998**, *98*, 2599.
[23] K. Weiss, G. Beernink, F. Dötz, A. Birkner, K. Müllen, C. H. Wöll, *Angew. Chem.* **1999**, *111*, 3974; *Angew. Chem. Int. Ed.* **1999**, *38*, 3748.
[24] S. Peter, W. Tin, *Liebigs Ann. Chem.* **1983**, *3*, 519.
[25] P. Jakob, D. Menzel, *Surf. Sci.* **1988**, *201*, 503.
[26] P. Jakob, D. Menzel, *Langmuir* **1991**, *7*, 134.
[27] H. Koschel, G. Held, H.-P. Steinrück, *Surf. Sci.* **2000**, *454*, 83.
[28] P. Jakob, A. Cassuto, D. Menzel, *Surf. Sci.* **1987**, *187*, 407.
[29] M. A. Barteau, J. Q. Broughton, D. Menzel, *Appl. Surf. Sci.* **1984**, *19*, 92.
[30] D. N. Denzler, C. Frischkorn, C. Hess, M. Wolf, G. Ertl, *Phys. Rev. Lett.* **2003**, *91*, 226102.
[31] W. H. Weinberg, *Acc. Chem. Res.* **1996**, *29*, 479.
[32] K. K. Onchoke, C. M. Hadad, P. K. Dutta, *J. Phys. Chem. A* **2006**, *110*, 76.
[33] E. A. Carrasco, M. Campos-Vallette, P. Leyton, G. Diaz, R. E. Clavijo, J. V. Garcia-Ramos, N. Inostroza, C. Domingo, S. Sanchez-Cortes, R. Koch, *J. Phys. Chem. A* **2003**, *107*, 9611.
[34] M.-C. Wu, D. W. Goodman, *J. Am. Chem. Soc.* **1994**, *116*, 1364.
[35] R. G. Greenler, *J. Chem. Phys.* **1966**, *44* 310.
[36] A. Braun, N. Shah, F. E. Huggins, G. P. Huffman, S. Wirick, C. Jacobsen, K. Kelly, A. F. Sarofim, *Fuel* **2004**, *83*, 997.
[37] A. Braun, N. Shah, F. E. Huggins, K. E. Kelly, A. Sarofim, C. Jacobsen, S. Wirick, H. Francis, J. Ilavsky, G. E. Thomas, G. P. Huffman, *Carbon* **2005**, *43*, 2588.

